Electron Nuclear Double Resonance (ENDOR) of the $Q_c^{\bullet-}$ Ubisemiquinone Radical in the Mitochondrial Electron Transport Chain†

John C. Salerno and Marcy Osgood
Department of Biology, Center for Biophysics, Rensselaer Polytechnic Institute, Troy, New York 12180
Yajun Liu, Harold Taylor, and Charles P. Scholes*
Department of Physics, Center for Biochemistry and Biophysics, State University of New York at Albany, Albany, New York 12222
Received October 31, 1989; Revised Manuscript Received March 7, 1990

ABSTRACT: We present an electron nuclear double resonance (ENDOR) study of the bound $Q_c^{\bullet-}$ ubisemiquinone in the mitochondrial quinol cytochrome *c* reductase complex. An ENDOR probe specifically modified for insertion into our electron paramagnetic resonance cavity was used for this study. We observed strongly hyperfine-coupled protons whose exchangeable nature indicated they were hydrogen-bonded to the quinone oxygen(s). It is thought that such hydrogen bonds are critical in binding the ubiquinone to protein, in stabilizing its semiquinone form, and in modulating the thermodynamic properties of the bound ubiquinone in the mitochondrial quinol cytochrome *c* reductase complex. Additional ENDOR features were assigned to protons of the quinone ring itself and to weakly coupled protons that may be associated with nearby amino acids. From very weakly hyperfine-coupled, distant, exchangeable protons there was also ENDOR evidence to suggest proximity and accessibility of the ubiquinone site to the solvent.

Mitochondrial quinol cytochrome *c* reductase (also called the cytochrome bc_1 complex) was the first bioenergetic complex to have a specific molecular model proposed for coupling vectorial transmembrane proton flux to electron transport (Mitchell, 1976). A major feature of the original and subsequent Q[1] cycles (Mitchell, 1976; Crofts & Meinhardt, 1982) was the necessity for quinone binding sites that effectively modify the thermodynamic properties of quinone. QCR is believed to contain two sites that bind ubiquinone, and QCR also contains cytochromes b_{566}, b_{562}, c_1, and the Rieske iron–sulfur center. One such site, labeled Q_c or Q_i, stabilizes the ubisemiquinone anion ($Q_c^{\bullet-}$) relative to its quinone and quinol forms and is sensitive to antimycin, which quenches the semiquinone radical of the Q_c site (Siedow et al., 1978; Ohnishi & Trumpower, 1980; Salerno & Ohnishi, 1980; De Vries et al., 1982; Ohnishi et al., 1982). With X-band (9 GHz) EPR, the $Q_c^{\bullet-}$ radical has a line width between derivative extrema of about 9 G and is readily power-saturated at liquid nitrogen temperatures (Salerno & Ohnishi, 1980). The other site, designated Q_z or Q_o, does not thermodynamically stabilize ubisemiquinone radical forms, but a radical identified with a ubisemiquinone bound at this site can be observed by electron paramagnetic resonance during turnover conditions *in* the presence of antimycin (De Vries et al., 1981). The inhibitor UHDBT hinders electron transfer at the "o" site without directly acting on Q_c. Q_c is widely believed to function as a site of ubisemiquinone reduction by using electrons recycled through the low-potential (*b* cytochrome) arm of QCR. Q_z is believed to be the site of quinol oxidation and to correspond to Mitchell's center o (Mitchell, 1976).

The effects of pH on the titration of the antimycin-sensitive $Q_c^{\bullet-}$ radical are complex (Robertson et al., 1984). The radical is stabilized at alkaline pH, as expected for an anionic semiquinone. Above pH 8 little further stabilization can be achieved, and the limiting maximum concentration of radical observed by EPR in oxidation–reduction titrations is only 0.4–0.5 spins per cytochrome c_1. Analysis of the data indicates that above pH 8 deprotonation of a group, presumably associated with a polypeptide component of the binding site, occurs except in the presence of $Q_c^{\bullet-}$; i.e., protonation of the polypeptide group favors binding of $Q_c^{\bullet-}$. Above pH 8 the pH dependences of the quinone/semiquinone and semiquinone/quinol couples are effectively equal, and the stability constant of the semiquinone is nearly independent of pH and of order unity (Robertson et al., 1984).

The thermodynamic coupling through the effective p*K* of this polypeptide group to the redox state of bound $Q_c^{\bullet-}$ has suggested a close physical association between the proton on this group and $Q_c^{\bullet-}$. Although this proton cannot be so closely bound to the $Q_c^{\bullet-}$ oxygen that it produces a neutral semiquinone EPR spectrum [whose EPR line width would be 11–12 G (Hales & Case, 1981)], it may still interact strongly enough to be a major factor in stabilizing the radical state, $Q_c^{\bullet-}$. Application of ENDOR spectroscopy should provide evidence for such potentially significant proton(s) magnetically hyperfine coupled to the stabilized radical.

Succinate cytochrome reductase (SCR) also contains an additional site of semiquinone stabilization, Q_s, which is the input point for electrons from succinate dehydrogenase (Ruzicka et al., 1975; Konstantinov & Ruuge, 1977). This

† This research was supported by U.S. Public Health Service Grants GM 34306 (J.C.S.), GM 35103 (C.P.S.), and RR 0712221 (C.P.S.) and by American Heart Association Grant 881041 (C.P.S.).
* Author to whom correspondence should be addressed.

[1] Abbreviations: EPR, electron paramagnetic resonance; ENDOR, electron nuclear double resonance; χ', dispersion; χ'', absorption; ν_{ENDOR}, the ENDOR frequency; ν_{NMR}, the free proton NMR frequency; RF, radiofrequency; G, gauss (1 gauss = 10^{-4} tesla); FM, frequency modulation; T_1, spin–lattice relaxation time; RC, bacterial reaction center; CTPO, 3-carbamoyl-2,2,5,5-tetramethyl-3-pyrrolin-1-yloxy free radical; DPPH, 2,2-diphenyl-1-picrylhydrazyl radical; ptp, peak to peak; o.d., outer diameter; i.d., inner diameter; TTFA, 1-thienoyl-3,3,3-trifluoroacetone; UHDBT, 6-hydroxy-5-undecyl-4,7-benzothiazoledione; Bicine, *N*,*N*-bis(2-hydroxyethyl)glycine; QCR, quinol cytochrome *c* reductase; SCR, succinate cytochrome *c* reductase, which is a complex of succinate quinone reductase and QCR; Q, quinone.

0006-2960/90/0429-6987$02.50/0

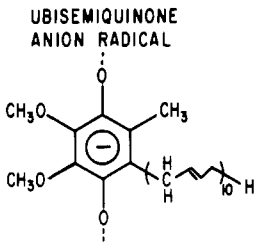

larger SCR complex is composed of quinol cytochrome *c* reductase and succinate quinone reductase. The $Q_s^{\bullet-}$ radical stabilized at this site can be readily distinguished from $Q_c^{\bullet-}$ because it is sensitive to different inhibitors and because, unlike $Q_c^{\bullet-}$, it exhibits rapid spin relaxation (Salerno & Ohnishi, 1980). $Q_s^{\bullet-}$ is antimycin and UHDBT insensitive, but it is quenched by TTFA-type inhibitors (Ingledew et al., 1976).

In a biochemical setting ubisemiquinone has been most extensively studied in bacterial reaction centers of *Rhodopseudomonas viridis* (Deisenhofer et al., 1985) and *Rhodobacter sphaeroides* (Allen et al., 1987a,b), whose three-dimensional structure is known to 2.6-Å resolution. ENDOR has probed the tightly bound primary quinone "Q_A^-" and the more loosely bound, secondary "Q_B^-" in the reaction center of *Rb. sphaeroides*. The data from these centers on weakly and strongly hyperfine-coupled protons, both exchangeable and nonexchangeable, are a useful set for comparison with the present results.

The bacterial reaction center of *Rb. sphaeroides* has a molecular weight of about 10^5 and can be prepared for magnetic resonance at a protein concentration of 100 μM. The ubisemiquinone radicals in it, especially Q_A^-, can be obtained in nearly 100% abundance (M. Okamura, private communication) because they have a high stability constant compared to those of the quinone and quinol forms (O'Keefe et al., 1982) and because they can be created by photolysis. Photosynthetic reaction centers can withstand embedding in Langmuir–Blodgett films (Alegria et al., 1985) and study in organic solvents (Warncke et al., 1989). On the other hand, SCR and QCR are more difficult to work with; to obtain optimum concentrations of ubisemiquinone they must be redox poised under proper pH conditions. In relatively dilute suspensions, about 0.4 $Q_c^{\bullet-}$ spins per cytochrome c_1 can be obtained at pH 8.5 (Robertson et al., 1984), but at high protein concentrations it is difficult to exceed 0.25 $Q_c^{\bullet-}$ spins per cytochrome c_1. Even highly concentrated (100 μM) suspensions of these complexes are magnetically quite dilute for ENDOR of $Q_c^{\bullet-}$.

Our goal has been to optimize the ENDOR signal from this dilute paramagnetic system. Previous ENDOR on quinones of reaction centers used high RF power and temperatures above liquid nitrogen (Feher et al., 1985; Lubitz et al., 1985). We thus modified our preexisting system (Scholes, 1979), originally designed for liquid helium ENDOR, to function at nitrogen temperatures. For free radical systems that have relatively mobile side groups (e.g., CH_3 side chains) and long relaxation times, nitrogen temperatures, rather than helium, lead to better resolution of ENDOR features at moderate (milliwatt) microwave powers.

Experimental Procedures

ENDOR Apparatus. Our present system is based on an ER-420 Bruker EPR spectrometer with low power and dispersion capability. The EPR–ENDOR cavity was a homemade TE 102 cavity (Van Camp et al., 1976) that was located inside a set of double dewars, and there were 100-kHz field-modulation coils wound directly adjacent to the EPR cavity within the cryogenic space. Although this cavity was designed

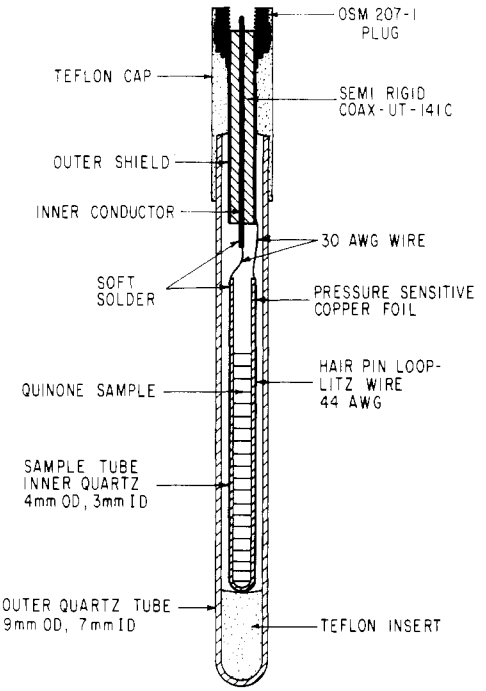

FIGURE 1: ENDOR insert probe used for quinone work. The probe consists of a 4-mm o.d., 3-mm i.d. quartz sample tube with vertically wound RF loop made of Litz wire. The wire of the loop is fed by coax from the RF power amplifier. The sample tube sits inside a larger 7-mm i.d., 9-mm o.d. quartz tube. The entire combination of tubes is attached to the end of a coaxial wand and inserted inside our EPR cavity.

for ENDOR at liquid helium temperatures where the ENDOR coil was wrapped about the outside of the cavity, for the present application we designed the higher power ENDOR insert probe shown in Figure 1. We developed a simple ENDOR insert that would accommodate moderate size (0.2 mL) EPR samples and an RF coil configured for higher RF fields at the sample than in the previous helium system. The ENDOR coil, in the form of a hairpin turn, was vertically looped about the inner 4-mm o.d., 3-mm i.d. quartz sample tube. The probe[2] was designed for easy insertion into the EPR cavity *with coil inside the EPR cavity and within 1–2 mm of the sample*, ready removal via an SMA plug from its coaxial feed, and easy cryogenic storage. The ENDOR probe was positioned within the EPR cavity for an optimal cavity quality factor of about 1000, a condition that occurred when the plane of the loop was the plane of minimum microwave E field. The RF source was a Hewlett-Packard 8601A frequency generator whose output was fed to a 100-W Electronic Navigation Inc. amplifier and thence to the ENDOR coax. The voltage output ramp from our signal averager was used to sweep the 8601A over the desired frequency range while the ENDOR-induced changes were synchronously stored in the memory of the signal averager. At room temperature the ENDOR RF current was estimated by a Tektronix CT-2 current probe attached next to the RF coil and in series with it. The RF magnetic field, which can be computed from this current and the known dimension of the coil, gave at 15 MHz a 4-G ptp RF amplitude at the center of the sample tube when we used the same RF

[2] Recently loop gap resonators, first originated by Froncisz and Hyde (1981), have been developed by R. A. Isaacson of the Feher group for study of small (30 μL) but concentrated samples of photosynthetic reaction centers. The loop gap resonator is ideal for such physically small but magnetically concentrated samples. Where spin concentration is small but sample size is not a limitation, as with our system, the loop gap resonator is not an advantage (R. A. Isaacson, personal communication).

amplifier output as applied for ENDOR. Over the 10–20-MHz range there was a monotonic increase in RF current by approximately a factor of 2.

With this system we could do field-modulated ENDOR as previously done at helium temperatures (Scholes, 1979) but have an order of magnitude higher RF field. With field-modulated ENDOR we used dispersion (χ'), adiabatic rapid passage where the field-modulated EPR signal is sensitive to changes in effective relaxation rates brought on by ENDOR transitions. With the field-modulated ENDOR we directly detected the RF-induced changes in the EPR signal, whereas with frequency-modulated ENDOR, one obtains the derivative of the RF-induced changes. If there is adequate signal-to-noise, the absorption derivative presentation [$(d\chi''/d\nu_{ENDOR})$ vs ν_{ENDOR}] previously used on more concentrated quinone model systems (O'Malley & Babcock, 1984a,b, 1985, 1986) and reaction centers (Feher et al., 1985; Lubitz et al., 1985) can yield more spectral detail but at the expense of sensitivity. Although frequency-modulated ENDOR certainly works with our insert probe on more concentrated radical systems, we have found that the needed ENDOR sensitivity on our weak quinone samples is attained with field modulation under rapid passage conditions (Scholes, 1979).

Materials. By the methods of Yu and Yu (1980, 1982), QCR was prepared from beef heart mitochondria as part of the larger SCR complex. The SCR is a more intact preparation than QCR alone and does not require replenishment of quinone or lipid (Yu & Yu, 1980, 1982). Experiments were also conducted with phospholipid- and quinone-replenished QCR. While similar radical species were observed, the intensity of the EPR signals in the SCR preparation was higher; for this reason we chose to use the SCR for this initial ENDOR study. SCR was suspended in 0.1% sodium cholate to an approximate protein concentration of 25 mg/mL and a cytochrome c_1 concentration of 75 μM. The samples were poised with a 50:1 fumarate–succinate mixture (redox potential of −14 mV) at pH 8.5 in Bicine buffer for 5 min and then transferred to the ENDOR probe and frozen in liquid nitrogen. This redox poise discriminates against flavin radicals, which have a different EPR line shape from $Q^{\bullet-}$ radicals in any case (Ohnishi et al., 1981). The deuterated sample was dialyzed overnight vs two changes of 99.9% deuterated buffer and then allowed to react with the fumarate–succinate poising mixture and also frozen. Due to the proximity of the $Q_s^{\bullet-}$ radical of SCR to paramagnetic metal centers (Salerno & Ohnishi, 1980), $Q_s^{\bullet-}$ will not readily microwave power saturate at liquid nitrogen temperatures. Furthermore, the paramagnetic metal centers themselves in any of these complexes will not microwave saturate at liquid nitrogen temperature. If an EPR signal will not saturate, one cannot obtain an ENDOR signal from it. We have not used liquid helium temperatures for these ubiquinone studies in order to avoid complication from underlying heme and iron–sulfur protein ENDOR signals, which do emerge at liquid helium temperatures.

For preliminary ENDOR tests and as a concentration standard in EPR integrations, we used a 100 μM CTPO sample dissolved in 1:1 water–ethylene glycol. For preliminary ENDOR tests on a commonly available quinone, we used a *p*-benzoquinone sample whose semiquinone form was prepared by air oxidation of a 10 mM *p*-benzoquinol solution in slightly basic ethanol (O'Malley & Babcock, 1984a,b). Double integration of the EPR signal indicated a concentration of about 60 μM for *p*-benzosemiquinone anion. From protons of *p*-benzosemiquinone, the rapid passage ENDOR spectra (included as supplementary material) yielded large couplings of

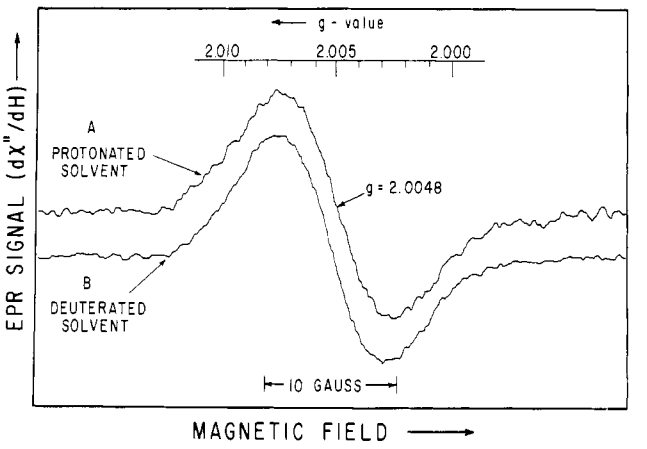

FIGURE 2: EPR spectra of the $Q_c^{\bullet-}$ radical in protonated (A) and deuterated (B) media recorded at 90 K with microwave power of 30 μW and 100-kHz field modulation of approximately 2.2 G ptp. Each spectrum was the result of 32 accumulations of 20 s each over a 50-G range with an experimental time constant of 0.02 s. *g*-factors were determined by comparison with a DPPH sample of known 2.0036 *g*-value, where appropriate small corrections were made for small differences in EPR frequency and magnetic field between the sample and DPPH. For a comparison of line shape, the spectra here were normalized to the same ptp height.

2.5 ± 0.2, 5.6 ± 0.3, and 9.1 ± 0.7 MHz to be respectively compared with the couplings of 2.5 ± 0.3, 6.2 ± 0.3, and 9.5 ± 0.3 MHz reported by O'Malley & Babcock (1984b) on the same system. These workers used frequency-modulated ENDOR from a standard Bruker ER 200D EPR–ENDOR system at 123 K. The exact position and shape of such features will be sensitive to the EPR line position (O'Malley & Babcock, 1986) due to orientation selection arising from *g*-anisotropy.

Results

Figure 2 shows the EPR spectra of the $Q_c^{\bullet-}$ radical from SCR protein suspended in the protonated and the deuterated buffers, respectively. These spectra are shown normalized to the same peak-to-peak derivative height for a detailed comparison of line shape. Before normalization, the integrated intensity of the signal from the deuterated sample was about 30% higher than that of the protonated sample. *g*-values were calibrated by reference to a DPPH sample with a known *g*-value of 2.0036 ± 0.0003 (Poole, 1983). We doubly integrated these spectra and compared results with the doubly integrated spectrum of CTPO; from these integrations we estimate that there were 10–15 μM ubisemiquinone spins in these samples.

EPR spectra of samples of SCR poised under the conditions described for the ENDOR samples indicated that the slowly relaxing semiquinone signal shown in Figure 2 was quenched by antimycin but not by UHDBT or TTFA (data not shown). At high levels of microwave power (>10 mW) some $Q_s^{\bullet-}$ radical could be observed, but since $Q_s^{\bullet-}$ is not saturated (Salerno & Ohnishi, 1980), it could not contribute to the ENDOR spectrum under the conditions described. The EPR line shape, saturation properties, redox properties, and inhibitor sensitivity characteristics unambiguously identified the slowly relaxing radical as $Q_c^{\bullet-}$, the stabilized semiquinone identified with the site of Q reduction in QCR.

A proton will typically yield an ENDOR spectrum that is a pair of features centered at the free proton NMR frequency, ν_{NMR}, and split away from this frequency by $\pm A/2$, where A is the hyperfine coupling.

$$\nu_{ENDOR} = \nu_{NMR} \pm A/2 \quad (1)$$

Table I: Proton Hyperfine Couplings from This Paper[a]

features	figure	couplings (MHz)	behavior on H/D exchange	assignment
1, 1′	3A	4.0 ± 0.4	exchanges, leaving 4, 4′	$A_\perp$ component of proton(s) hydrogen-bonded to quinone oxygen(s)
4, 4′	3B	3.9 ± 0.7	remains after H/D exchange	possibly $A_\perp$ component of quinone CH_3 or CH_2 (not well resolved)
2, 2′	3A	8.4 ± 0.5	outer part of 2, 2′ undergoes H/D exchange	$A_\parallel$ component of protons hydrogen-bonded to quinone oxygen(s)
3, 3′	3B	7.8 ± 0.7	remains after H/D exchange	$A_\parallel$ component from quinone CH_3 or CH_2
α, α′	4A–C	0.20 ± 0.05	no exchange	amino acid protons or distant quinone protons
β, β′	4A,B	0.75 ± 0.1	no exchange	
γ, γ′	4C	1.1 ± 0.1	no exchange	
feature at ν_{NMR}	4A–C	<0.1	partial H/D exchange	exchangeable protons >5 Å distant from quinone

[a] At 90 K.

A reflects both the isotropic contact coupling due to unpaired s electron density actually on the proton and anisotropic dipolar couplings. The dipolar coupling[3] has a $1/r^3$ dependence, where r is the distance between the electron spin and the position of the proton.

These are frozen solution spectra, and in a frozen solution or a powder the different orientations of the semiquinone will cause a spread in proton ENDOR frequencies with some buildup of ENDOR intensity at the principal values ($A_\parallel$ and especially $A_\perp$) of the hyperfine tensor (Feher et al., 1985). If there is some underlying g-anisotropy, it may be possible to select particular orientations of hyperfine tensors by selecting a particular g-value on the EPR line. In this case a component of the hyperfine tensor collinear with the g-tensor may be enhanced (Feher et al., 1985; O'Malley & Babcock, 1986). We did observe such dependence with the weakly coupled protons (Figure 4), but we still need better signal-to-noise to resolve such orientation dependence from the strongly coupled protons (Figure 3) at g-values away from the EPR line center.

We expect to observe pairs of proton ENDOR lines centered on the free proton NMR frequency (of about 14.7 MHz for this work). Some pairs cluster near the free proton frequency, and these clustered features are due to weakly coupled protons ($A < 2$ MHz) not immediately adjacent to the radical. There will also be strongly hyperfine-coupled protons with ENDOR features that occur several megahertz away from the free proton frequency. These may be methyl or methylene protons attached to the quinone ring or protons directly hydrogen-bonded to the quinone oxygens (Lubitz et al., 1985; Feher et al., 1985; O'Malley & Babcock, 1984a,b, 1985, 1986). Values for the hyperfine couplings to such protons from photosynthetic and model systems given in Table II.

In field-modulated dispersion ENDOR we often have seen a sharp dip at the free proton frequency (Scholes, 1979). The depth and extent of this dip can be altered by deuteration of the solvent. A proton ENDOR signal occurring at or very near the free proton frequency has been called a "matrix" ENDOR signal. (The term "matrix ENDOR" should not be confused here with the term "matrix side" or inside of the mitochondrial membrane.) Kevan and Kispert (1976, section 4.6.2) have shown by theory and experiment on model paramagnetic systems that proton matrix ENDOR depends on protons which are weakly dipole coupled to the electron spin and which are within the local environment of an unpaired spin, typically within 5–6 Å. When a matrix ENDOR signal changes on deuteration, the reason is that the radical site is accessible to those exchangeable protons which provide the matrix ENDOR signal (Kevan & Kispert, 1976, p 240).

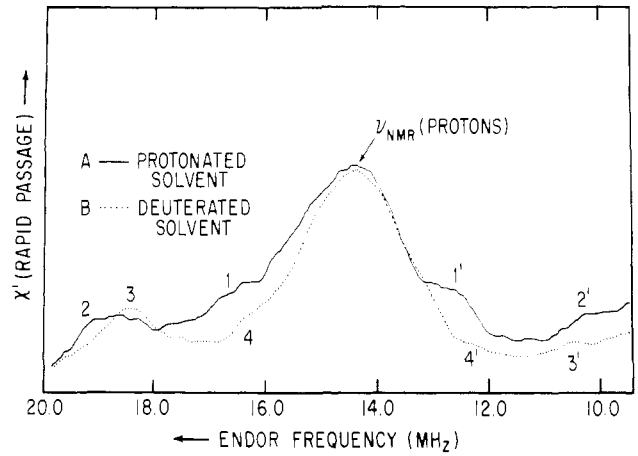

FIGURE 3: Comparison of the ENDOR spectra from $Q_c^{\bullet-}$ in (A) protonated (solid trace) and (B) deuterated (dotted trace) solvent over an 8–20-MHz frequency range. Spectra were run in the dispersion rapid passage mode with 1-mW microwave power and a 100-kHz field modulation of 0.45 G ptp. The frequency range was swept in a time of 0.5 s. The protonated spectrum represented 9000 accumulations, and the deuterated spectrum represented 13 000 accumulations. The RF field at the sample was approximately 4 G ptp. Each spectrum was taken at the center of the EPR line at the $d\chi''/dH$ zero crossing. Features labeled 1, 1′ are from exchangeable protons; 2, 2′ appear to be from a compendium of exchangeable and nonexchangeable protons; and 3, 3′ are from nonexchangeable protons. ν_{NMR} was approximately 14.7 MHz, and the EPR frequency was 9.72 GHz. Temperature of samples was approximately 90 K.

The ENDOR spectra of the protonated and deuterated $Q_c^{\bullet-}$ samples, taken over the range of 8–20 MHz with the magnetic field on the center of the EPR line, are shown in Figure 3, traces A and B, respectively. The couplings of such features, their behavior under H/D exchange, and their assignments are given in Table I. The resolution of strongly coupled features, e.g., 1, 1′, with coupling of order 4 MHz, was best obtained with a field modulation of 0.45 G ptp and with rapid (24 MHz/s) frequency sweeps.[4] The most significant difference between samples prepared with protonated vs deuterated solvent was in the pronounced shoulders labeled 1, 1′ in the protonated sample; the hyperfine coupling of these features is 4.0 ± 0.4 MHz. Upon deuteration there emerged

[3] A first-order point dipole approximation for the hyperfine coupling of an electron to a proton is $hA_{dipole} = g_{eff}\beta_e g_n \beta_n (3\cos^2\theta - 1)/r^3$, where g_{eff} is the electronic g-value, β_e is the electronic Bohr magneton, β_n is the nuclear Bohr magneton, g_n is the nuclear g-value = 5.58, θ is the angle between the applied magnetic field and the vector between the electron spin and the proton, r is the unpaired electron to proton distance, and h is Planck's constant.

[4] The intensity of the strongly coupled proton ENDOR signal can be enhanced by superimposing a small 1-kHz FM on the ENDOR RF source through an available feature on the HP 8601A frequency generator (Van Camp et al., 1981). The magnitude of the FM deviation was 75 kHz. We did not use this 1-kHz FM for first derivative detection but simply for enhancing the ENDOR signal amplitude. For the more detailed spectra near the free proton frequency we did not use this FM feature either, since it broadens narrow ENDOR features.

Table II: Proton Hyperfine Couplings from the Work of Others

exchangeable protons hydrogen-bonded to quinone oxygens	
Q_A of RC[a]	$A_\perp$ = 6.4 and 4.2 MHz; $A_\parallel$ = 9.0 MHz (at 123 K)
Q_B of RC[a]	$A_\perp$ = 5.0 and 3.1 MHz (at 123 K)
benzoquinone in 2-propanol[b]	$A_\perp$ = 2.8 MHz; $A_\parallel$ = 6.2 MHz (at 123 K)
ubiquinone in 2-propanol[b]	$A_\perp$ = 2.8 MHz; $A_\parallel$ = 6.1 MHz (at 123 K)
quinone CH_3 ring protons	
Q_A of RC[a]	$A_\perp$ = 4.1 MHz; $A_\parallel$ = 7.2 MHz (at 123 K)
Q_B of RC[a]	$A_\perp$ = 4.7 MHz; $A_\parallel$ = 7.9 MHz (at 123 K)
duroquinone in ethanol[c]	$A_\perp$ = 4.4 MHz; $A_\parallel$ = 7.5 MHz (at 123 K)
quinone isoprenoid CH_2	
Q_A of RC[a]	$A_\perp$ = 5.1 MHz; $A_\parallel$ = 8.4 MHz (at 123 K)
ubiquinone in liquid[a] dimethoxyethane	A_{iso} = 3.72 MHz, and A_{iso} = 2.06 MHz (at 205 K)[d]
weak couplings of nonexchangeable protons from protein near Q_A^{-}[e]	0.26, 0.51, 1.13, 1.9, 2.6 MHz (at 123 K)

[a] Feher et al., 1985. [b] O'Malley & Babcock, 1985. [c] O'Malley & Babcock, 1984a. [d] A_{iso} is the hyperfine coupling measured for a freely tumbling radical in solution. $A_{iso} = (A_\parallel + 2A_\perp)/3$. [e] Lubitz et al., 1985.

a less intense underlying set of features, 4, 4', which had about a 3.9-MHz splitting; these 4, 4' features did not have the general appearance of the 1, 1' features. In the 18–19-MHz region near but nonidentical peaks, labeled 2 from the protonated sample and 3 from the deuterated sample, were observed. There also were weak features, 2' from the protonated sample and 3' from the deuterated, in the 10–11-MHz region; these are possibly the lower frequency partners of the features 2 and 3, respectively.[5] If so, features 2, 2' have a coupling of 8.4 ± 0.5 MHz and 3, 3' have a coupling of 7.8 ± 0.7 MHz.

The weakly coupled proton spectra are shown in Figure 4. Resolution and ENDOR intensity of weakly coupled protons with couplings <2 MHz are enhanced by relatively slow (5 MHz/s) ENDOR frequency sweeps and with low (0.15 G ptp) field modulation. In the spectra of both the protonated and deuterated samples, Figure 4, traces A and B, respectively, there were peaks (α, α') with splittings of about 0.20 ± 0.05 MHz and shoulders (β, β') with couplings of 0.75 ± 0.1 MHz. The dip at the free proton frequency, ν_{NMR}, was sharper and deeper in the spectrum of the protonated sample. ENDOR intensity extended to greater than ±0.5 MHz away from the free proton frequency. When we took an ENDOR spectrum 4 G above the EPR line center, we took advantage, as in Figure 4, trace C, of the small g-anisotropy of the ubisemiquinone [$g_\perp$ = 2.006, $g_\parallel$ = 2.002 (Feher et al., 1972)] in resolving anisotropic hyperfine features (Feher et al., 1985; O'Malley & Babcock, 1986). Thus new features γ,γ' appeared with splitting of 1.1 ± 0.1 MHz and in both protonated and deuterated media.

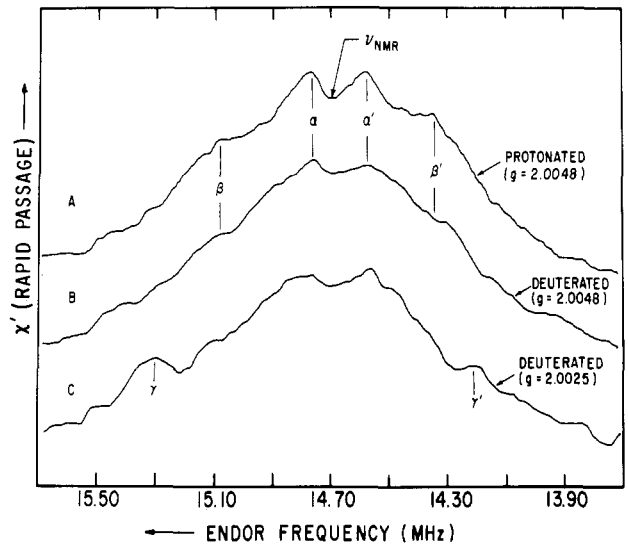

FIGURE 4: Proton ENDOR spectra taken over a 2-MHz range near the free proton frequency of 14.70 MHz to bring in weakly coupled protons. Rapid passage dispersion conditions were used, the microwave power was approximately 1 mW, and the 100-kHz field modulation was 0.15 G ptp. Each spectrum represented approximately 10000 0.5-s accumulations. Spectra A and B were taken at the EPR line center where $d\chi''/dH = 0$, while spectrum C was taken 4 G to higher field to show evidence for anisotropy in proton hyperfine couplings. Temperature of the samples was approximately 90 K.

Discussion

The EPR line shape in Figure 2, which is highly consistent with the previously reported X-band line shape of ubisemiquinone anion from bacterial reaction centers (Feher et al., 1972), is not perceptibly perturbed at X-band by deuteration. This lack of perturbation occurs because the line width of the ubisemiquinone radical is primarily due to unresolved g-anisotropy, not exchangeable protons. The g-anisotropy of $g_\perp$ = 2.006, $g_\parallel$ = 2.002 (Feher et al., 1972) translates into a line width contribution of at least 7 G at X-band (9.72 GHz here). There was no evidence for unwanted flavin radicals.

The major finding of this work was the ENDOR-detectable, exchangeable proton resonances 1, 1' with couplings of order 4 MHz. This finding of features 1, 1' is strong evidence for hydrogen bonding to the $Q_c^{\bullet-}$ ubiquinone. As previously reported from bacterial reaction centers (Feher et al., 1985) and from semiquinone model systems in protic alcoholic solvent (O'Malley & Babcock, 1985, 1986), such a coupling is in the range expected from the $A_\perp$ component of exchangeable protons hydrogen bonded to the oxygen(s) of semiquinone anions. (See Table II.) The outlying features 2, 2' at 18–19 and 9–10 MHz, respectively, appear also to have a contribution from exchangeable protons. Compared to the coupling of 8.4 MHz from 2, 2' here, the $A_\parallel$ component of hyperfine coupling to the exchangeable proton(s) was reported to have a value of 9 MHz from Q_A^- of the photosynthetic reaction center (Feher et al., 1985) and 6 MHz in model quinones in alcoholic solvent (O'Malley & Babcock, 1985).

The ENDOR information on strongly coupled exchangeable protons is definitive information that the $Q_c^{\bullet-}$ ubisemiquinone interacts through hydrogen bonds with its surroundings and

[5] For strongly coupled protons of both ubiquinone here and metal systems like Cu_A of cytochrome c oxidase (Van Camp et al., 1978), we found that the higher frequency partner of the proton pair predicted in eq 1 was more intense than the lower frequency partner. Such an intensity difference may be due to the competing effects on ENDOR transition probability from direct RF-induced nuclear transitions and from RF-induced modulation of the hyperfine coupling (Kevan & Kispert, 1976, section 1.4.3). The fact that the RF current here was a factor of 2 higher at 20 MHz than at 10 MHz is also an important consideration.

that the protons of these bonds are exchangeable with aqueous medium. This ENDOR study thus gives direct evidence for *exchangeable* protons at a redox moiety that has been proposed to couple transmembrane electron and proton flow (Mitchell, 1976).

To relate the dipolar electron–proton hyperfine coupling to oxygen–proton distances, Feher et al. (1985) combined the ENDOR data from the exchangeable, oxygen-bound protons of Q_A^- and Q_B^- with theoretical and experimental evidence on spin density at quinone oxygens. A 1.55–1.97-Å range of quinone oxygen–proton distances was determined. Given the similarity of couplings from the exchangeable proton(s) of $Q_c^{\bullet-}$, we would suggest a similar 1.5–2.0-Å oxygen–proton distance is likely. It seems probable that the strongly coupled site-derived protons are a major factor in the stabilization of the $Q_c^{\bullet-}$ radical. Electrostatic, hydrogen-bonding interactions over ~2 Å could be strong enough to account for the binding, which produces $Q_c^{\bullet-}$ stabilization, of the semiquinone $Q_c^{\bullet-}$ form relative to quinone and quinol forms. Weakly coupled exchangeable protons discussed below, if site-derived, could also participate to a lesser degree in the stabilization.

If there is more than one strongly coupled, exchangeable proton, it will be difficult to select a single tightly coupled proton as the "Robertson proton" (Robertson et al., 1984). In fact it is possible that the behavior attributed from thermodynamic considerations to this species arises from a combination of more than one strongly thermodynamically coupled proton. All potential strongly coupled protons need not be present at the same site at the same time; it is possible that interactions between ionizable groups do not allow the protonation of all such groups simultaneously. The ENDOR spectra of both Q_A^- and Q_B^- in reaction centers yielded two distinguishable exchangeable proton couplings that perhaps indicated different hydrogen bonds to the two quinone oxygens in both Q_A^- and Q_B^- (Feher et al., 1985). The resolution of these separate features was enhanced by the availability of deuterated quinone and deuterated reaction centers, which were then suspended in protonated solvent. From our present ENDOR study it is not yet obvious how many strongly hyperfine-coupled exchangeable protons are actually involved per $Q_C^{\bullet-}$, and hence we are not ready at this time to compare the details of quinone oxygen-to-hydrogen bonding in $Q_c^{\bullet-}$ to those in Q_A^- and Q_B^-. From a functional standpoint, the $Q_c^{\bullet-}$ semiquinone form is less stable than the Q_A^- or Q_B^- species (O'Keefe et al., 1982; Wraight et al., 1982), and this implies that the binding of a semiquinone anion, while still greatly favored over quinone or quinol forms, is less favored at the Q_c site than at Q_A or Q_B.

Our work also has shown evidence for stronger hyperfine couplings to nonexchangeable protons, notably features labeled 3, 3′ in the deuterated sample. Judging from the similarity of their hyperfine couplings to those reported for ubisemiquinone in models and reaction centers (Table II), these are from the $A_\parallel$ feature of the methyl or methylene isoprenoid protons on the quinone. The 3.9-MHz coupling of the weak features 4, 4′ would be of the same order as couplings of the $A_\perp$ feature methyl or methylene isoprenoid protons on the quinone, but our assignment of the weak 4, 4′ features remains tentative.

The small couplings α, α', β, β', γ, and γ' indicated in Figure 4 are of the same order as weak electron–proton hyperfine couplings in bacterial reaction centers. In the reaction centers these couplings, which did not disappear on deuteration of solvent or ubiquinone, were evidently couplings to neighboring amino acid protons (Lubitz et al., 1985). The couplings reported here are not precisely those found in the bacterial reaction centers, however, probably because the polypeptide environment of the ubiquinone here is different from that in the bacterial reaction centers. From the difference in spectral features obtained at different g-values (Figure 4, B vs C), we have evidence for hyperfine anisotropy in at least some of these couplings, and this anisotropy indicates a dipolar character to the coupling. The g-value where the features γ, γ' in Figure 4C were obtained is known to be perpendicular to the quinone ring (Hales & Case, 1981), and a crude estimate of a hypothetical proton-to-quinone distance could be made under the assumption that the electron spin is located at the center of the quinone and the proton of interest is directly above or below the quinone so that $\theta = 0°$. (See footnote 3.) Then a coupling of 1.1 MHz would yield a distance of 5.3 Å from quinone center to proton. Proton-to-quinone distances of the order 4–6 Å are probably appropriate for the weakly coupled protons that give rise to couplings of features α, α', β, β', γ, and γ' although a detailed distance estimate from dipolar couplings should include the delocalized character of the electron spin (Feher et al., 1985; O'Malley & Babcock, 1986). We believe that study of these weakly coupled protons and of their perturbation by redox phenomena or genetic manipulation will give insight into how the protein environment modulates the redox properties of the ubiquinone in the QCR complex (Siedow et al., 1978).

The Q_c site is believed to be on the inside or matrix side of the mitochondrial membrane (Crofts et al., 1987). The proton matrix ENDOR feature at the free proton ENDOR frequency, ν_{NMR}, which diminishes on deuteration, gives at least qualitative information that the $Q_c^{\bullet-}$ center may be accessible to the bulk solvent. Several proteins with flavin radicals have shown ~50% reduction in matrix proton ENDOR in D_2O, and this reduction implies accessibility of the flavin radical to solvent (Kevan & Kispert, 1976, section 7.1.1). When a matrix ENDOR signal changes on deuteration, the reason is that the radical site is accessible at a distance >5–6 Å to exchangeable protons which provide the matrix ENDOR signal (Kevan & Kispert, 1976, section 4.6.2). Since access to solvent is important for a proton-translocating moiety like ubiquinone, we believe that the origins and details of this very weakly coupled ENDOR signal should be studied.

Supplementary Material Available

The rapid passage ENDOR spectrum of p-benzosemiquinone and its accompanying figure legend (2 pages). Ordering information is given on any current masthead page.

Registry No. $Q_c^{\bullet-}$, 27696-12-4; SCR, 9028-10-8.

References

Alegria, G., Dutton, P. L., Popovic, Z., & Kovacs, G. J. (1985) *Biophys. J. 47*, 4a.

Allen, J. P., Feher, G., Yeates, T. O., Komiya, H., & Rees, D. C. (1987a) *Proc. Natl. Acad. Sci. U.S.A. 84*, 5730–5734.

Allen, J. P., Feher, G., Yeates, T. O., Komiya, H., & Rees, D. C. (1987b) *Proc. Natl. Acad. Sci. U.S.A. 84*, 6162–6166.

Crofts, A., & Meinhardt, S. W. (1982) *Biochem. Soc. Trans. 10*, 201–203.

Crofts, A., Robinson, H., Andrews, K., Van Dorn, S., & Berry, E. (1987) in *Cytochrome Systems—Molecular Biology and Energetics* (Papa, S., Chance, B., & Ernster, L., Eds.) pp 617–624, Plenum Press, New York.

Deisenhofer, J., Epp, O., Miki, K., Huber, R., & Michel, H. (1985) *Nature (London) 318*, 618–624.

De Vries, S., Albracht, S. P. J., Berden, J. A., & Slater, E. C. (1981) *J. Biol. Chem. 256*, 11996–11998.

De Vries, S., Berden, J. A., & Slater, E. C. (1982) in *Function of Quinones in Energy Conserving Systems* (Trumpower, B. L., Ed.) pp 235–246, Academic Press, New York.

Feher, G., Okamura, M. Y., & McElroy, J. D. (1972) *Biochim. Biophys. Acta 267*, 222–226.

Feher, G., Isaacson, R. A., Okamura, M. Y., & Lubitz, W. (1985) in *Antennas and Reaction Centers of Photosynthetic Bacteria* (Michel-Beyerle, M. E., Ed.) Springer Series in Chemical Physics, Vol. 42, pp 174–189, Springer-Verlag, Berlin, West Germany.

Froncisz, W., & Hyde, J. S. (1982) *J. Magn. Reson. 47*, 515–521.

Hales, B. J., & Case, E. E. (1981) *Biochim. Biophys. Acta 637*, 291–302.

Ingledew, W. J., Salerno, J. C., & Ohnishi, T. (1976) *Arch. Biochem. Biophys. 177*, 176–184.

Kevan, L., & Kispert, L. D. (1976) *Electron Spin Double Resonance Spectroscopy*, Wiley, New York.

Konstantinov, A. A., & Ruuge, E. K. (1977) *FEBS Lett. 81*, 137–141.

Lubitz, W., Abresch, E. C., Debus, R. J., Isaacson, R. A., Okamura, M. Y., & Feher, G. (1985) *Biochim. Biophys. Acta 808*, 464–469.

Mitchell, P. (1976) *J. Theor. Biol. 62*, 327–367.

Ohnishi, T., & Trumpower, B. (1980) *J. Biol. Chem. 255*, 3278–3284.

Ohnishi, T., King, T. E., Salerno, J. S., Blum, H., Bowyer, J. R., & Maida, T. (1981) *J. Biol. Chem. 256*, 5577–5582.

Ohnishi, T., Salerno, J. C., & Blum, H. (1982) in *Function of Quinones in Energy Conserving Systems* (Trumpower, B. L., Ed.) pp 247–261, Academic Press, New York.

O'Keefe, D. P., Prince, R. C., & Dutton, P. L. (1982) in *Function of Quinones in Energy Conserving Systems* (Trumpower, B. L., Ed.) pp 271–276, Academic Press, New York.

O'Malley, P. J., & Babcock, G. T. (1984a) *J. Chem. Phys. 80*, 3912–3913.

O'Malley, P. J., & Babcock, G. T. (1984b) *J. Am. Chem. Soc. 106*, 817–818.

O'Malley, P. J., & Babcock, G. T. (1985) in *Antennas and Reaction Centers of Photosynthetic Bacteria* (Michel-Beyerle, M. E., Ed.) Springer Series in Chemical Physics, Vol. 42, pp 339–344, Springer-Verlag, Berlin, West Germany.

O'Malley, P. J., & Babcock, G. T. (1986) *J. Am. Chem. Soc. 108*, 3995–4001.

Poole, C. P., Jr. (1983) in *Electron Spin Resonance*, 2nd ed., p 443, Wiley, New York.

Robertson, D. E., Prince, R. C., Bowyer, J. R., Matsuura, K., Dutton, P. L., & Ohnishi, T. (1984) *J. Biol. Chem. 259*, 1758–1763.

Ruzicka, F., Beinert, H., Schefler, K., Dunham, R., & Sands, R. (1975) *Proc. Natl. Acad. Sci. U.S.A. 72*, 2886–2890.

Salerno, J. C., & Ohnishi, T. (1980) *Biochem. J. 192*, 769–781.

Scholes, C. P. (1979) in *Multiple Electron Resonance Spectroscopy* (Dorio, M., & Freed, J. H., Eds.) pp 297–328, Plenum Press, New York.

Siedow, J. N., Power, S., de la Rosa, F. F., & Palmer, G. (1978) *J. Biol. Chem. 253*, 2392–2399.

Van Camp, H. L., Scholes, C. P., & Isaacson, R. A. (1976) *Rev. Sci. Instrum. 47*, 516–517.

Van Camp, H. L., Wei, Y.-H., Scholes, C. P., & King, T. E. (1978) *Biochim. Biophys. Acta 537*, 238–246.

Van Camp, H. L., Sands, R. H., & Fee, J. A. (1981) *J. Chem. Phys. 75*, 2098–2107.

Warncke, K., & Dutton, P. L. (1989) *Biophys. J. 55*, 181a.

Wraight, C. A. (1982) in *Function of Quinones in Energy Conserving Systems* (Trumpower, B. L., Ed.) pp 181–197, Academic Press, New York.

Yu, C. A., & Yu, L. (1980) *Biochim. Biophys. Acta 591*, 409–420.

Yu, C. A., & Yu, L. (1982) *J. Biol. Chem. 257*, 2016–2021.